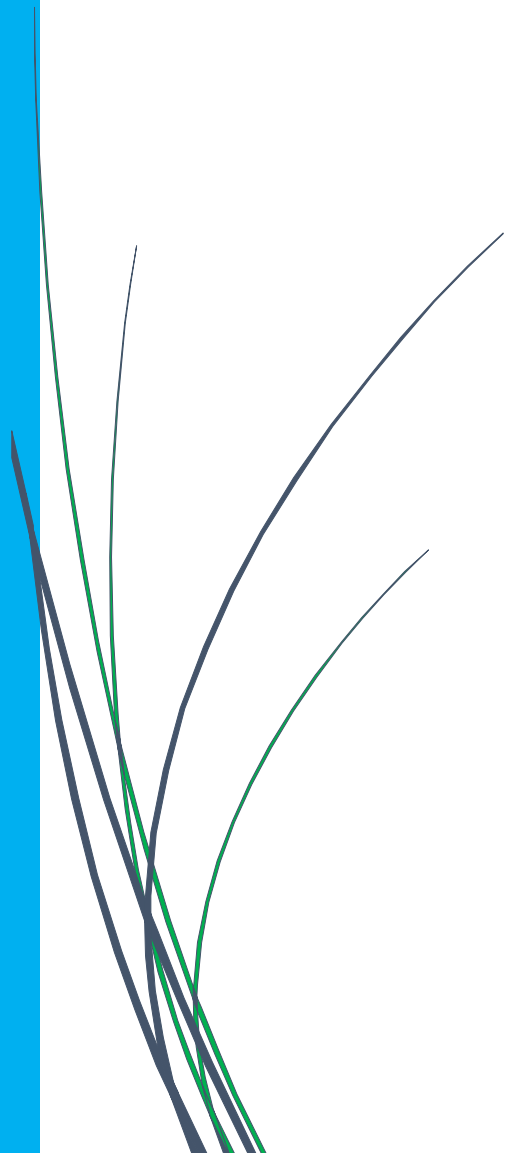


## Chapter:8

# Promising nano bimetallic oxides of Ni-Co/CeO<sub>2</sub> catalyst for ESR





## 8.1 Introduction

The solvothermal method involves the simultaneous effect of pressure and temperature with solvent. This exclusive synthesis method leads controlled morphology of nano particles for applications in various fields [122, 348, 349]. Nevertheless, these studies are still constrained up to the precipitation followed by solvothermal treatment, or the reaction among different species within hydrothermal or solvothermal treatment [342, 350-353]. Recently, Hammond et al.[354] synthesized the nano CeO<sub>2</sub> using Deep Eutectic Solvents reline and ethaline (1:2 ChCl: ethylene glycol) mixture by solvothermal treatment. But after solvothermal reaction, they found cloud like suspension, which get precipitated by treatment with water. The precipitation potential of a solvent for metal oxide through solvation of their precursor and solvothermal treatment is still not reported in the literature. The temperature and pH of the reaction medium have major role in precipitation reaction. In solvothermal treatment, pH cannot be controlled, but temperature can be varied. Since the properties of solution differ with pressure and temperature, it may result in different characteristics. The nano-size catalysts are very active for steam reforming of ethanol. The CeO<sub>2</sub> based support is highly active in steam reforming reactions because it has good oxygen mobility even during the reaction [355]. As reported in chapter 3, the synergistic effect of Ni and Co was found positive for ESR. Therefore, CeO<sub>2</sub> supported bimetallic Ni-Co catalysts were selected for further studies.

## 8.2 Experimental

### 8.2.1 Catalyst preparation

Four types of catalysts were prepared by solvothermal precipitation. The nomenclature of the catalysts is as follows: CeO<sub>2</sub>-SP, 20% Co/CeO<sub>2</sub> (Co/CeO<sub>2</sub>-SP), 20% Ni/CeO<sub>2</sub> (Ni/CeO<sub>2</sub>-SP) and 20%Ni-Co/CeO<sub>2</sub> (Ni-Co/CeO<sub>2</sub>-SP). For the preparation of CeO<sub>2</sub>, 0.25M solution (5.42 g Ce (NO<sub>3</sub>)<sub>2</sub>.6H<sub>2</sub>O solubilized in 50 ml of ethanol) was taken

in Teflon vessel of 200 ml, which was kept in autoclave reactor for different durations (2h, 4h and 6h) into the furnace at different temperature (373K, 393K, 413K, and 433K). After cooling at room temperature, the precipitate was separated by centrifugation at 14500 rpm for 5 minutes. The liquid part was decanted and the solid precipitate was dried at room temperature without washing to find out whether the nitrate impurities persist after precipitation or not. The XRD analysis of the precipitate confirmed that pure  $\text{CeO}_2$  was formed directly by solvothermal process (reported in section 8.3.1.3). The obtained  $\text{CeO}_2$  precipitate ( $\text{CeO}_2\text{-P}$ ) was calcined in a furnace at 673K for 3h. The calcination temperature was determined by thermo gravimetric analysis (TGA) of  $\text{CeO}_2\text{-P}$ .

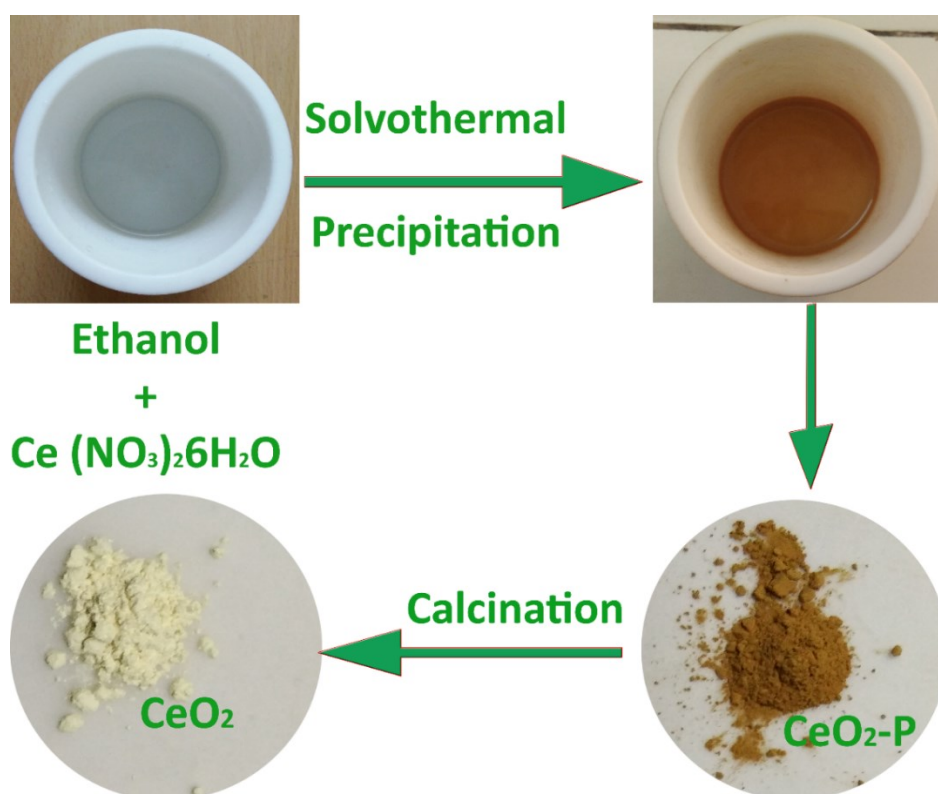


**Figure 8.1** The colour difference at difference stage of reactions.

The photographs of the precipitate before calcination and after calcination are shown in Figure 8.1. The color of dried precipitate before calcination was brown which turned yellowish-white after calcination. The color of the dried precipitate indicates that

some organic species may be present in the sample which was completely removed after calcination.

Similarly, 20%Co/CeO<sub>2</sub> and 20%Ni/CeO<sub>2</sub> were prepared by adding the stoichiometric amount of Ni (NO<sub>3</sub>)<sub>2</sub>.6H<sub>2</sub>O and Co (NO<sub>3</sub>)<sub>2</sub>.6H<sub>2</sub>O in the 0.25 M solution of Ce precursor individually. 20%Ni Co/CeO<sub>2</sub>-SP was prepared by mixing the stoichiometric concentration of Ni (NO<sub>3</sub>)<sub>2</sub>.6H<sub>2</sub>O, Co (NO<sub>3</sub>)<sub>2</sub>.6H<sub>2</sub>O and Ce (NO<sub>3</sub>)<sub>2</sub>.6H<sub>2</sub>O in 50ml ethanol. The mixture was taken in Teflon vessel of 200 ml, which was kept in autoclave reactor at optimized temperature and duration (obtained after CeO<sub>2</sub> precipitation). The obtained precipitate of catalysts were calcined at 823K for 3h because the maximum temperature of ESR performance for this study was opt 823K.

The three bimetallic catalysts having different compositions of 10, 15 and 20% Ni-Co/CeO<sub>2</sub> were prepared by co-precipitation cum solvothermal precipitation method. The percentage of Ni-Co was equivalent to NiCo<sub>2</sub>O<sub>4</sub>. First of all, the NiCo<sub>2</sub>O<sub>4</sub> was prepared by co-precipitation method was described elsewhere [356]. In brief, the aqueous solution of both precursors (Ni (NO<sub>3</sub>)<sub>2</sub>.6H<sub>2</sub>O and Co (NO<sub>3</sub>)<sub>2</sub>.6H<sub>2</sub>O) were prepared in 1:2 (Ni: Co) molar ratio and precipitated with the help of 150 ml KOH (1M) solution under vigorous stirring and N<sub>2</sub> bubbling condition. The precipitated blue colour mixture was continuously stirred for 6h and then separated by centrifugation at 5000 rpm. The hot distilled water was used for washing three times and then dried in oven overnight. The calcination of mixture was done at 623K for 21h. Next, a part of the prepared NiCo<sub>2</sub>O<sub>4</sub> was added in required amount into the ethanol solution of Ce (NO<sub>3</sub>)<sub>2</sub>.6H<sub>2</sub>O. The ultrasonication of the slurry was performed for dispersion for 15 minutes. Then, the slurry was kept in Teflon vessel of 200 ml, in autoclave reactor for 4h into the furnace at 413K. After cooling at room temperature, the slurry was centrifuged at 14500 rpm for 5 min. The obtained solid was calcined at 773K for 2h.

### 8.2.2 ESR performance Test

ESR reaction was performed in vertical quartz reactor having internal diameter 9 mm. 100 mg of catalyst was kept on quartz wool bed prepared at center of the reactor. The effect of different stoichiometric ratio of water and ethanol (3:1, 6:1 and 12:1) was also studied. The feed rate of ethanol water mixture was kept constant 4ml/h. The time on stream experiment was performed over the optimized reaction conditions.

## 8.3 Results and discussion

### 8.3.1 Characterization of catalyst

#### 8.3.1.1 Textural characterization

The textural properties surface area and pore volume of the catalysts are listed in table 8.1. It is apparent from the table that the specific surface area and pore volume both reduced with increasing Ni-Co concentration. It may be due to blocking of some pores of CeO<sub>2</sub> by Ni-Co. Meanwhile, the surface area and pore volume data of Co/CeO<sub>2</sub>-SP, Ni/CeO<sub>2</sub>-SP and Ni-Co/CeO<sub>2</sub>-SP catalysts show that the catalysts prepared by solely solvothermal method have higher specific surface area and pore volume compared to the precipitation cum solvothermal method.

**Table 8.1** Surface area and pore volume of CeO<sub>2</sub> as well as CeO<sub>2</sub> supported catalysts

Catalyst	Surface Area (m <sup>2</sup> /g)	Pore Volume (ml/g)
CeO <sub>2</sub>	95.2	0.048
Ni/CeO <sub>2</sub> -SP	78.3	0.047
Co/CeO <sub>2</sub> -SP	64.1	0.038
NiCo <sub>2</sub> O <sub>4</sub>	47.5	0.025
10 Ni-Co/CeO <sub>2</sub>	63.2	0.037
15 Ni-Co/CeO <sub>2</sub>	50.4	0.028
20 Ni-Co/CeO <sub>2</sub>	35.9	0.026
20 Ni-Co/CeO <sub>2</sub> -SP	45.1	0.029

#### 8.3.1.2 Thermal analysis of precipitate

The TGA-DSC analysis of CeO<sub>2</sub>-P shown in Figure 8.2 revealed that the whole process of decomposition was completed in two steps. The initial weight loss 2% upto

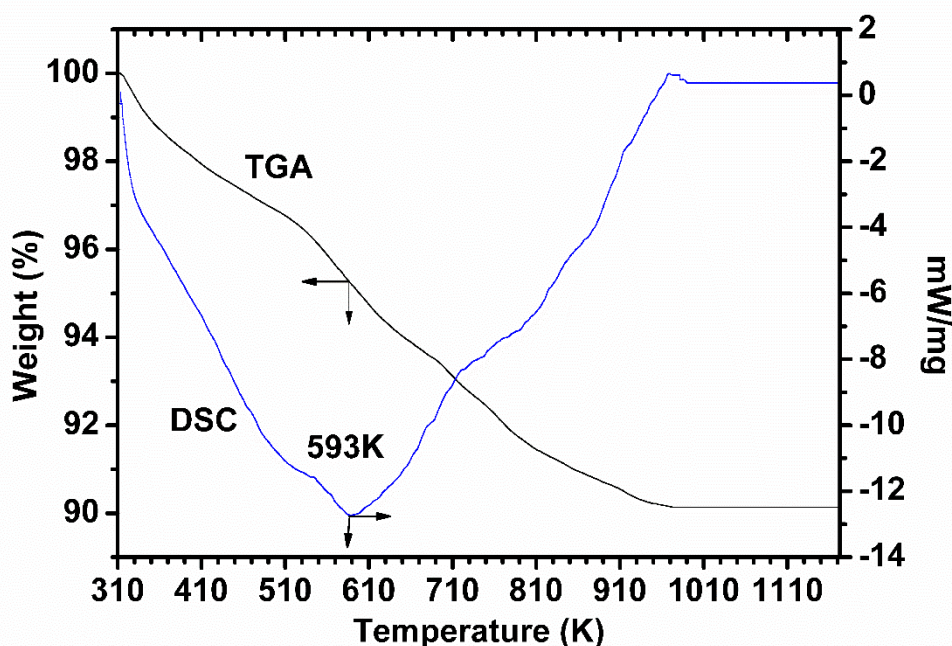


**Figure 8.2** TGA-DSC analysis graph of  $\text{CeO}_2$ -P with temperature.

393K in the first step may be due to surface adsorbed moisture. In the second step, the major weight losses of 8% occurred within 498-950K. The decomposable species present in the sample get lost below 950K. The DSC curve confirmed the endothermic process during complete weight loss. The weight loss may be due to decomposition of ethoxide, carbonate and crotonaldehyde species present in the sample, confirmed from ATR-FTIR analysis.

### 8.3.1.3 XRD analysis

The XRD pattern of the precipitate formed by solvothermal process ( $\text{Ce}(\text{NO}_3)_2 \cdot 6\text{H}_2\text{O} + \text{C}_2\text{H}_5\text{OH}$ ) is depicted in Figure 8.3. The  $2\theta$  values of the precipitate were  $28.54^\circ$  (111),  $33.07^\circ$  (200),  $47.47^\circ$  (220),  $56.33^\circ$  (311),  $59.07^\circ$  (222),  $69.40^\circ$  (400),  $76.68^\circ$  (331) and  $79.06^\circ$  (420) which confirmed that the face centered cubic crystallite of  $\text{CeO}_2$  was formed directly by solvothermal process (JCPDS 81-0792). The diffractogram does not show any other peak, and it indicates that the  $\text{CeO}_2$  was synthesized in pure form.

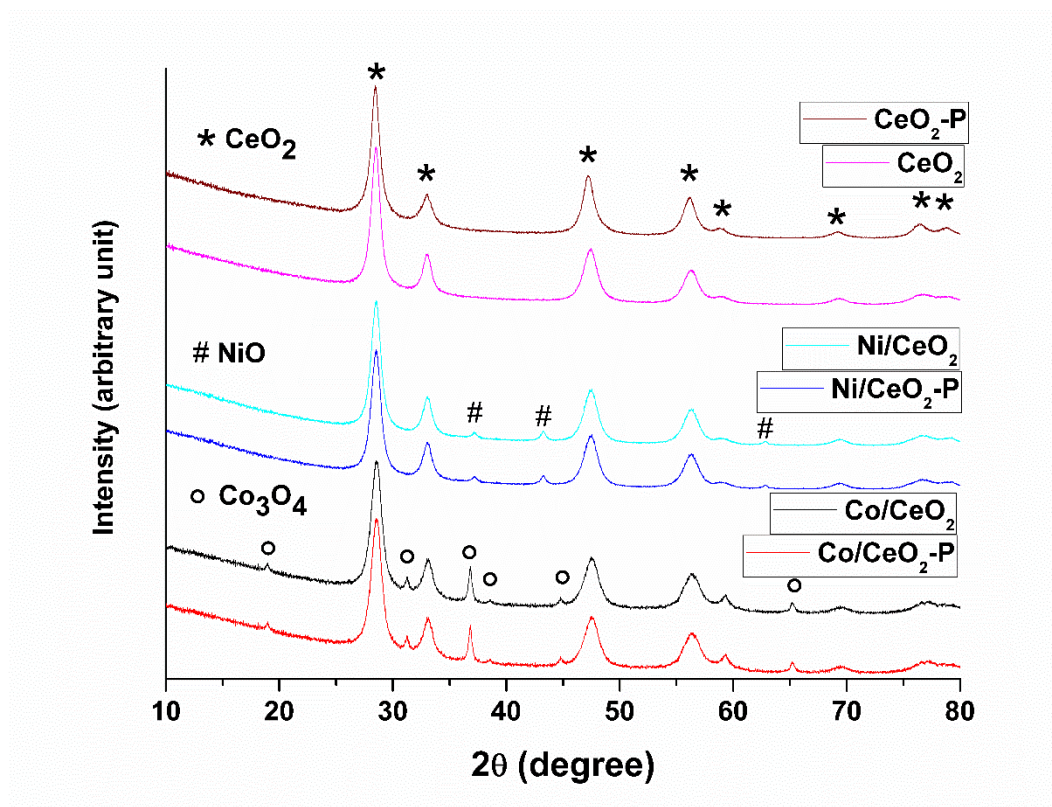


**Figure 8.3** HR-XRD of  $\text{CeO}_2$ ,  $20\text{Ni/CeO}_2\text{-SP}$ ,  $20\text{Co/CeO}_2\text{-SP}$  from top to bottom.

For  $\text{Ni/CeO}_2\text{-SP}$  and  $\text{Co/CeO}_2\text{-SP}$  samples XRD pattern revealed that along with  $\text{CeO}_2$ ,  $\text{NiO}$  and  $\text{Co}_3\text{O}_4$  were also formed respectively.

The XRD pattern of  $\text{NiCo}_2\text{O}_4$ ,  $10\text{Ni-Co/CeO}_2$ ,  $15\text{Ni-Co/CeO}_2$ ,  $20\text{Ni-Co/CeO}_2$ , and  $20\text{Ni-Co/CeO}_2\text{-SP}$  are presented in Figure 8.4. The  $2\theta$  values  $19.06^\circ$  (111),  $31.38^\circ$  (220),  $36.97^\circ$  (311),  $38.68^\circ$  (222),  $44.97^\circ$  (400),  $59.58^\circ$  (511),  $65.49^\circ$  (440) correspond with cubic and face-centered crystallite of  $\text{Co}_3\text{O}_4$  JCPDS (65-3103). The XRD pattern of  $\text{Ni/CeO}_2$  has shown the face centred cubic phase of  $\text{NiO}$  at  $2\theta$  value  $37.39^\circ$ ,  $43.24^\circ$  and  $62.70^\circ$  were matched with JCPDS (47-1049). The  $\text{NiCo}_2\text{O}_4$  spinel prepared by co-precipitation method consisted of face centred cubic crystallite at  $2\theta$  values  $18.92^\circ$  (111),  $31.15^\circ$  (220),  $36.70^\circ$  (311),  $38.40^\circ$  (222),  $44.63^\circ$  (400),  $55.43^\circ$  (422),  $59.13^\circ$  (511) and  $64.97^\circ$  (440) are in according to JCPDS (73-1702).

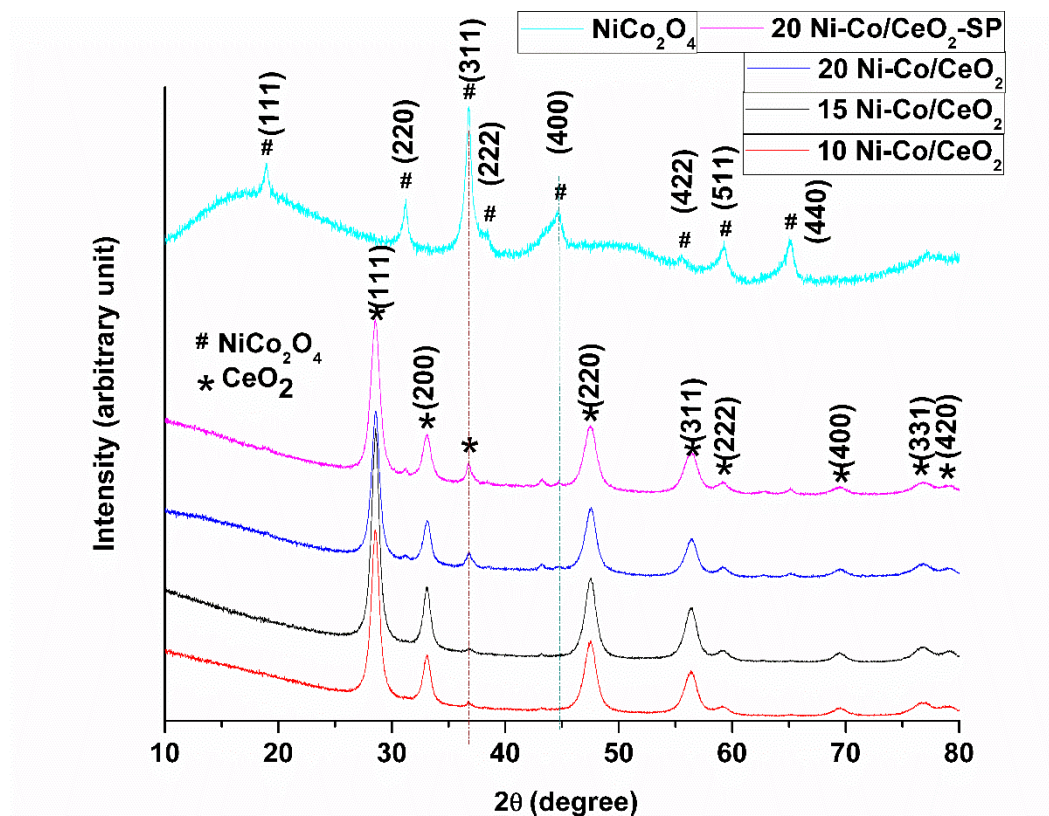


**Figure 8.4** HR-XRD of  $\text{NiCo}_2\text{O}_4$ ,  $20\text{Ni-Co/CeO}_2\text{-SP}$ ,  $20\text{Ni-Co/CeO}_2$ ,  $15\text{Ni-Co/CeO}_2$ , and  $10\text{Ni-Co/CeO}_2$  from top to bottom.

When ethanolic solution of  $\text{Ce}(\text{NO}_3)_2 \cdot 6\text{H}_2\text{O}$  was added into solid  $\text{NiCo}_2\text{O}_4$  (spinel) and treated solvothermally, the spinel structure of  $\text{NiCo}_2\text{O}_4$  disappeared. Similarly, it can be visualized from the diffractograms that no formation of  $\text{NiCo}_2\text{O}_4$  spinel structure took place in all the samples containing  $\text{CeO}_2$ . In case of  $\text{Ni-Co/CeO}_2$  catalyst, concentration of  $\text{CeO}_2$  was 80%, therefore the peak of  $\text{Co}_3\text{O}_4$  and  $\text{NiCo}_2\text{O}_4$  overlapped with  $\text{CeO}_2$  at  $2\theta$  values  $36.97^\circ$  and  $59.58^\circ$ .

#### 8.3.1.4 FTIR analysis

Yee et al. studied effect of ethanol on the surface of  $\text{CeO}_2$  based catalysts by *in situ* FTIR spectroscopy [357, 358]. They reported that with increasing temperature carbonate species dominantly persist on  $\text{CeO}_2$  surface, while ethoxy and acetaldehyde species decomposed. The FTIR spectra of each precipitate obtained in this study was almost corresponding to the spectra obtained at 623K by Yee et al. [89] for  $\text{CeO}_2$  based

catalysts. It indicates that the adsorbed carbonate species with two vibrational symmetric modes (1419 and 1335) and one asymmetric mode (OCO) (1536) were dominantly found on surface of precipitated  $\text{CeO}_2$ . These are the surface adsorbed species, because the carbonate of Ce or other active metal was not confirmed in XRD spectra. Beside, those peaks, the small intense peaks of C-O species for ethoxide (1020 and 1048) and crotonaldehyde (1649) were also found. After calcination, all these peaks disappeared but small broad peaks remained at  $1330\text{ cm}^{-1}$  which can be assigned for Ce-O-Ce [359].

The FTIR of  $\text{Co/CeO}_2$  and  $\text{Ni/CeO}_2$  catalyst precursor obtained after solvothermal precipitation reaction have also common peaks with  $\text{CeO}_2$  at wavenumber  $1640\text{ cm}^{-1}$  and  $1419\text{ cm}^{-1}$ . However, peak at  $1536\text{ cm}^{-1}$  of  $\text{CeO}_2$  was shifted at  $1556\text{ cm}^{-1}$  for  $\text{Co/CeO}_2$  and  $\text{Ni/CeO}_2$ . This shifting might be due to influence of co-ordination between Ce and O with Ni or Co. After calcination, these peaks were disappeared and peak at  $1330\text{ cm}^{-1}$  was become prominent.

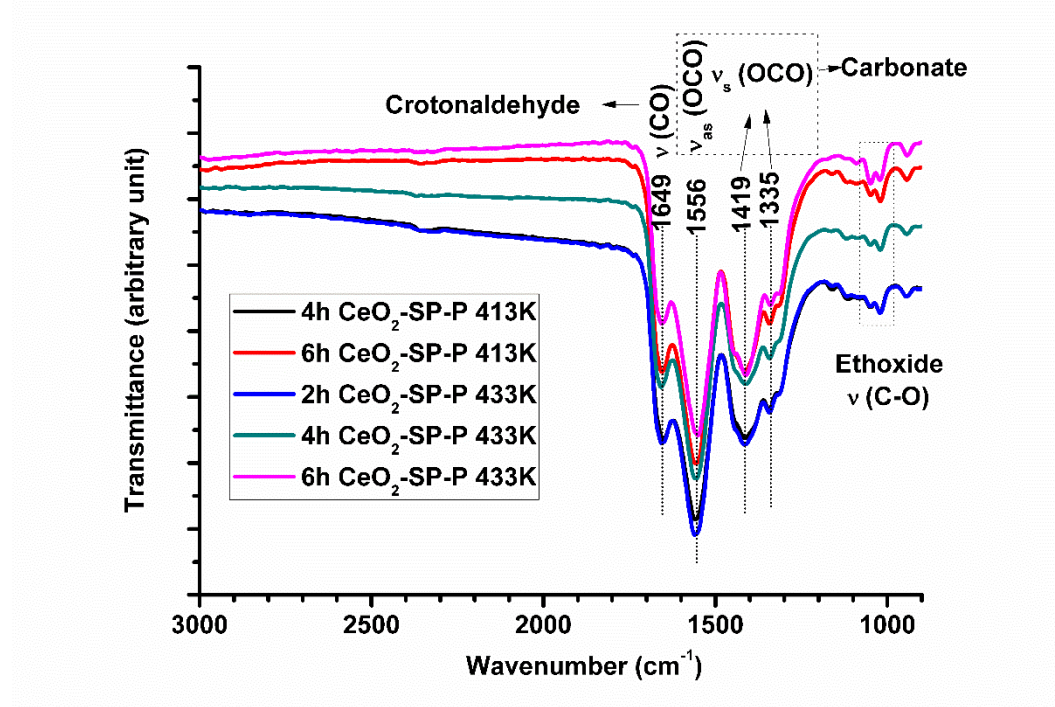


**Figure 8.5** ATR-FTIR of the  $\text{CeO}_2$ -SP-P after treatment with different temperature and time duration.

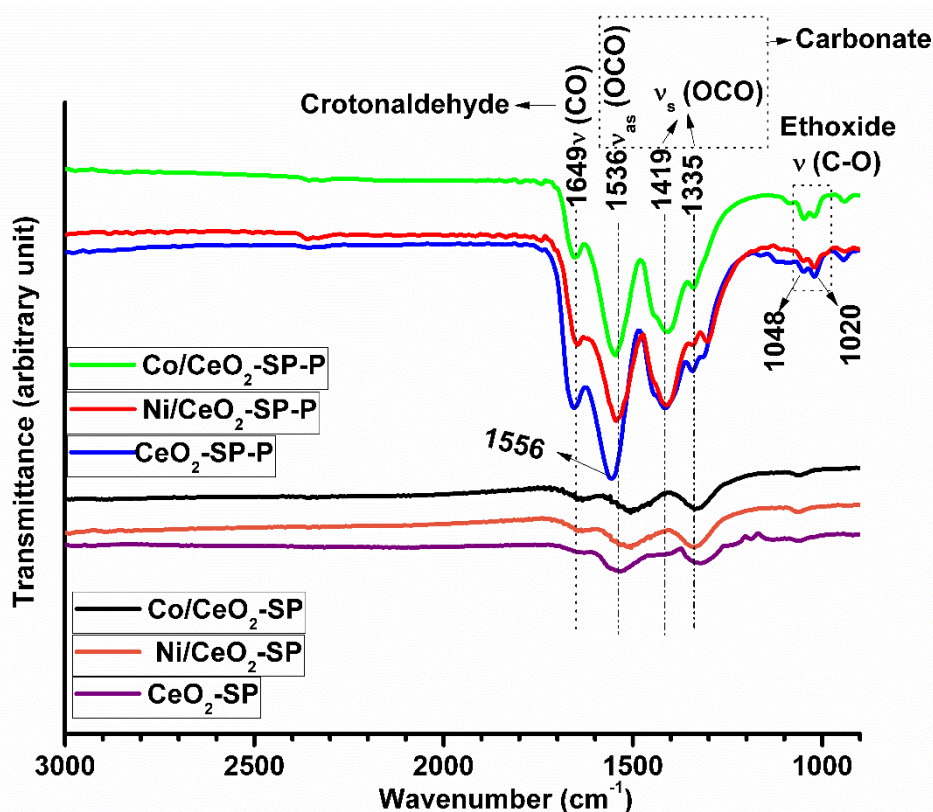


**Figure 8.6** ATR-FTIR of precipitate and their respective metal oxides.

The fingerprint region contains sharp peak at  $525\text{ cm}^{-1}$  for Ce-O bond. Hence,  $\text{CeO}_2$  formation was confirmed by an agreement of HR-XRD and FTIR data of prepared catalyst. The sharp peak at  $659\text{ cm}^{-1}$  and  $559\text{ cm}^{-1}$  can be assigned for  $\text{Co}_3\text{O}_4$ , whereas in case of  $\text{NiCo}_2\text{O}_4$   $655\text{ cm}^{-1}$  and  $553\text{ cm}^{-1}$ , the peak at  $655\text{ cm}^{-1}$  get shifted to  $662\text{ cm}^{-1}$  for each Ni-Co/ $\text{CeO}_2$  catalyst, which may be due to an interaction of Ni and Co with  $\text{CeO}_2$ . However, it is complicated to interpret the peaks after  $600\text{ cm}^{-1}$  for Ni-Co/ $\text{CeO}_2$  catalyst, because in that region the shoulder peak of  $\text{CeO}_2$  (about  $525\text{ cm}^{-1}$ ) with NiO and  $\text{Co}_3\text{O}_4$  got overlapped. It is clear from the figure that the peak intensity got reduced at  $659\text{ cm}^{-1}$  as compared to  $600\text{--}500\text{ cm}^{-1}$  region because of increase in concentration of  $\text{CeO}_2$ . The peak intensity was higher for  $10\text{Ni-Co/CeO}_2$  at wave number  $1330\text{ cm}^{-1}$ , but lowest at  $662\text{ cm}^{-1}$ , because the concentration of  $\text{CeO}_2$  is higher in  $10\text{Ni-Co/CeO}_2$  and concentration of NiO and  $\text{Co}_3\text{O}_4$  were higher in  $30\text{ Ni-Co/CeO}_2$ .

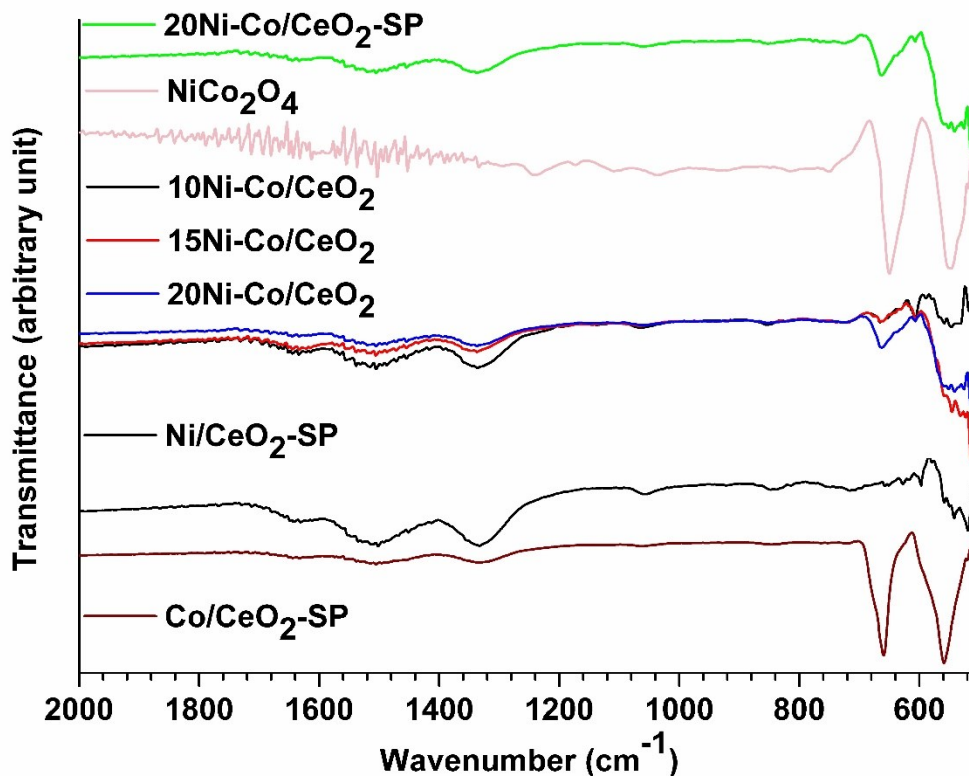


**Figure 8.7** Comparative ATR-FTIR of each bimetallic and mono metallic catalyst.

### 8.3.1.5 Morphology analysis

The Transmission electron microscope (TEM) imaging analysis of CeO<sub>2</sub>-SP is shown in Figure 8.8. The high-resolution images of CeO<sub>2</sub>-P and CeO<sub>2</sub> show the crystalline nature of particles with dominant (111) planes. From Figure 8.8a and 8.8b, the average particle size calculated using image J software for CeO<sub>2</sub>-P and CeO<sub>2</sub> were within 9.7-10 nm range. It is interesting to note that crystal development of CeO<sub>2</sub>-P occurred even before calcination. Even after calcination of CeO<sub>2</sub>-P at 413K, the nano-size particles remain intact. But calcination of CeO<sub>2</sub>-P at 433K produced three different forms (rod, cubic and hexagonal) of the particles with 95nm average particle size (Figure 8.8e and 8.8f). It indicates that nucleation of particles is higher with an increase in temperature during solvothermal treatment.

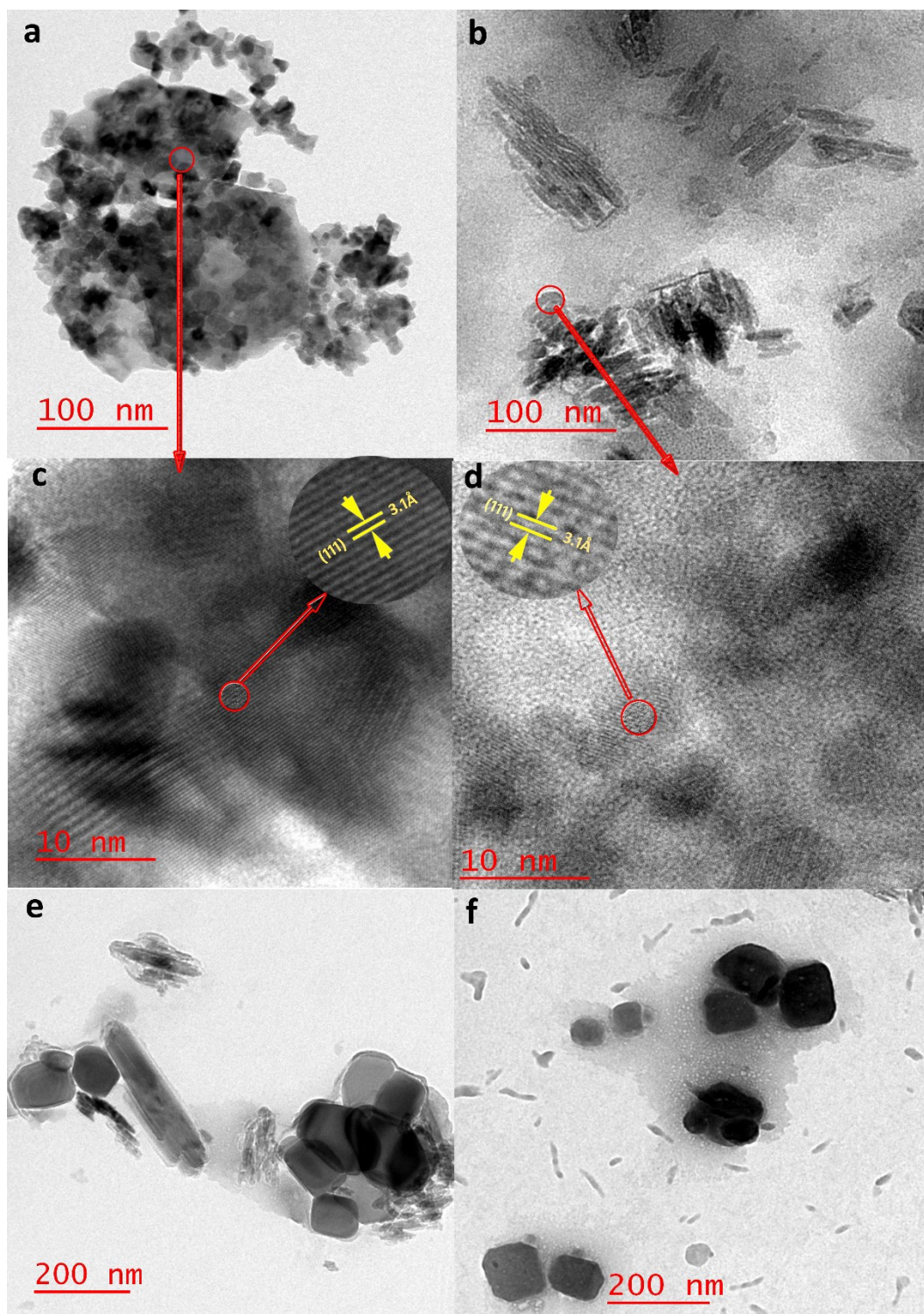


**Figure 8.8** TEM image of CeO<sub>2</sub>-SP-P(a), CeO<sub>2</sub>-SP (Solvothermal treatment at 413K for 4h ) (b), CeO<sub>2</sub>-SP (Solvothermal treatment at 413K for 6h ) (e and f) and HR-TEM image of CeO<sub>2</sub>-SP-P (c), CeO<sub>2</sub>-SP (d).

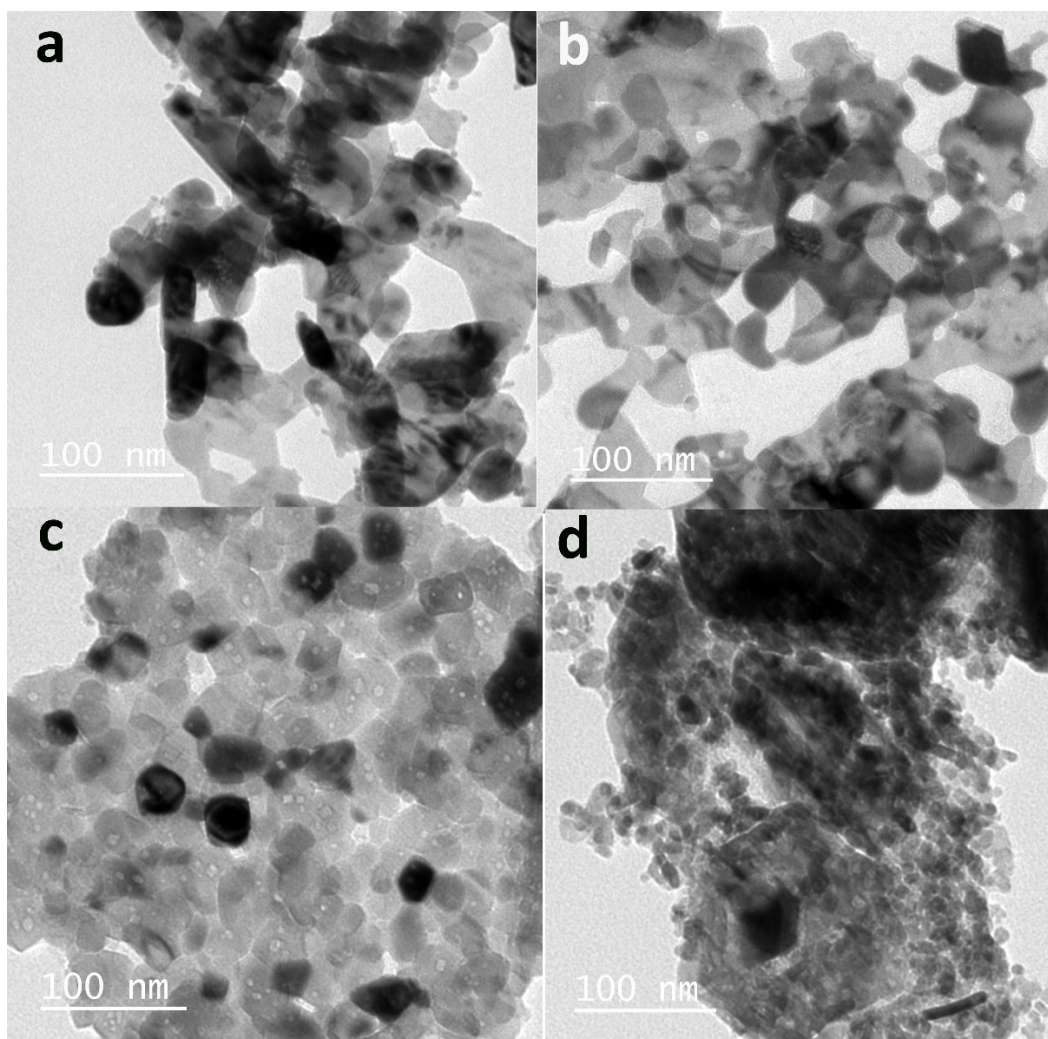


**Figure 8.9** TEM image of Ni/CeO<sub>2</sub>-SP (a), Co/CeO<sub>2</sub>-SP (b), 20Ni-Co/CeO<sub>2</sub>-SP (c), and 20Ni-Co/CeO<sub>2</sub> (d).

The TEM images of Co/CeO<sub>2</sub> and Ni/CeO<sub>2</sub> are also presented in Figure 8.9a and 8.9b respectively. The average particle size is 20-25 nm which is higher than CeO<sub>2</sub>. It may be due to high-temperature calcination of Co/CeO<sub>2</sub>-P and Ni/CeO<sub>2</sub>-P as compared to CeO<sub>2</sub>.

### 8.3.2 ESR performance test

ESR performance product distribution graph with ethanol conversion and selectivity of different gases versus temperature are presented in Figure 8.10. The product gas selectivity variation can be easily observed from the graph with respect to Ni-Co concentration. The ethanol conversion also increases with increasing concentration of

active metal catalyst. Independently, Ni shows less ethanol conversion compared to Co at lower temperature, but above 773K, the ethanol conversion was almost complete for each catalyst. In case of bimetallic catalyst with CeO<sub>2</sub>, the spinel form of catalyst didn't exist but the synergistic effect of Co and Ni resulted into almost constant ethanol conversion within 673-873K temperature. The double carbon content product selectivity was higher in Co/CeO<sub>2</sub> compared to Ni/CeO<sub>2</sub>. The C<sub>2</sub>H<sub>4</sub> and CH<sub>3</sub>CHO selectivity were reduced for each Ni-Co/CeO<sub>2</sub> catalyst.

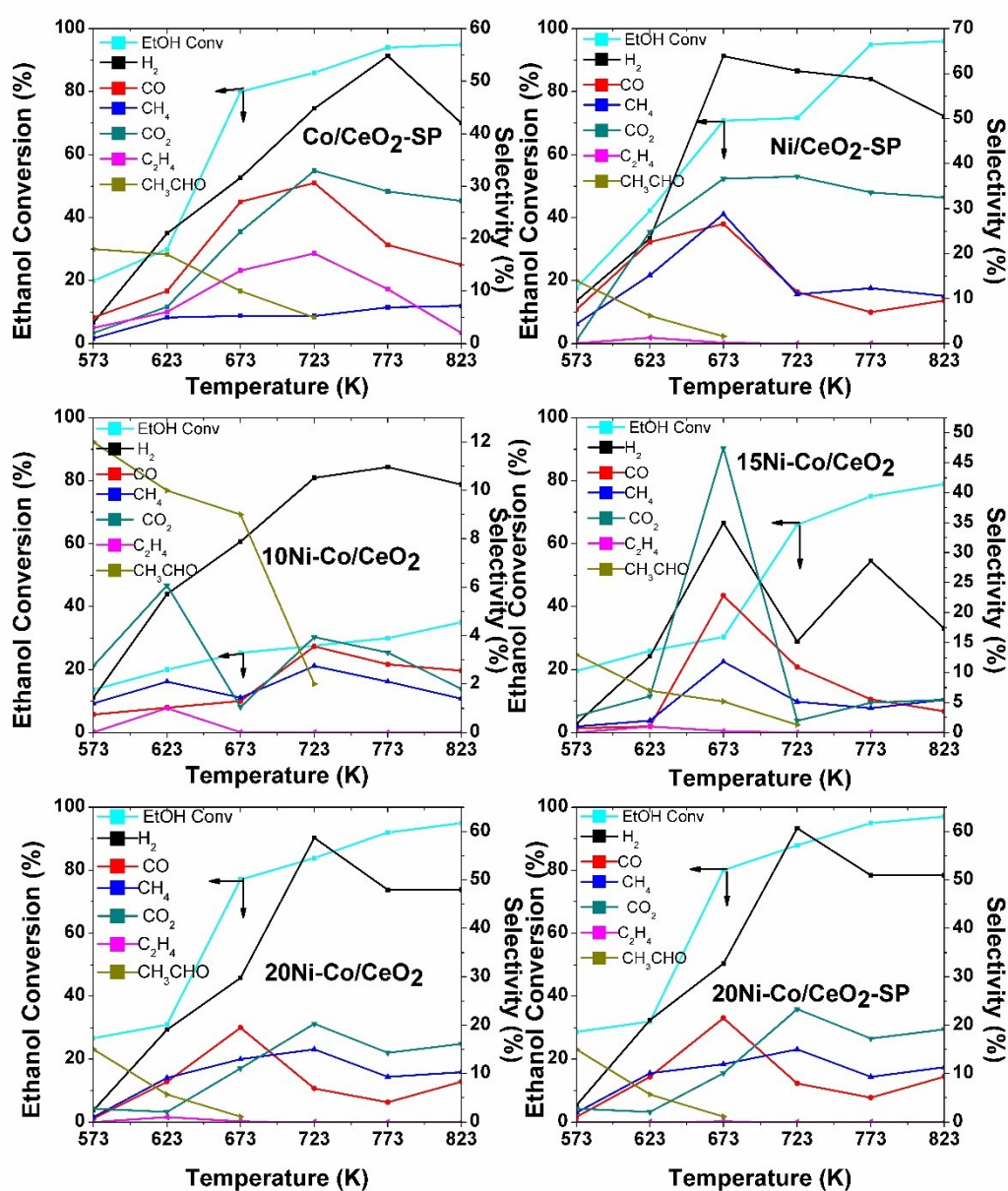
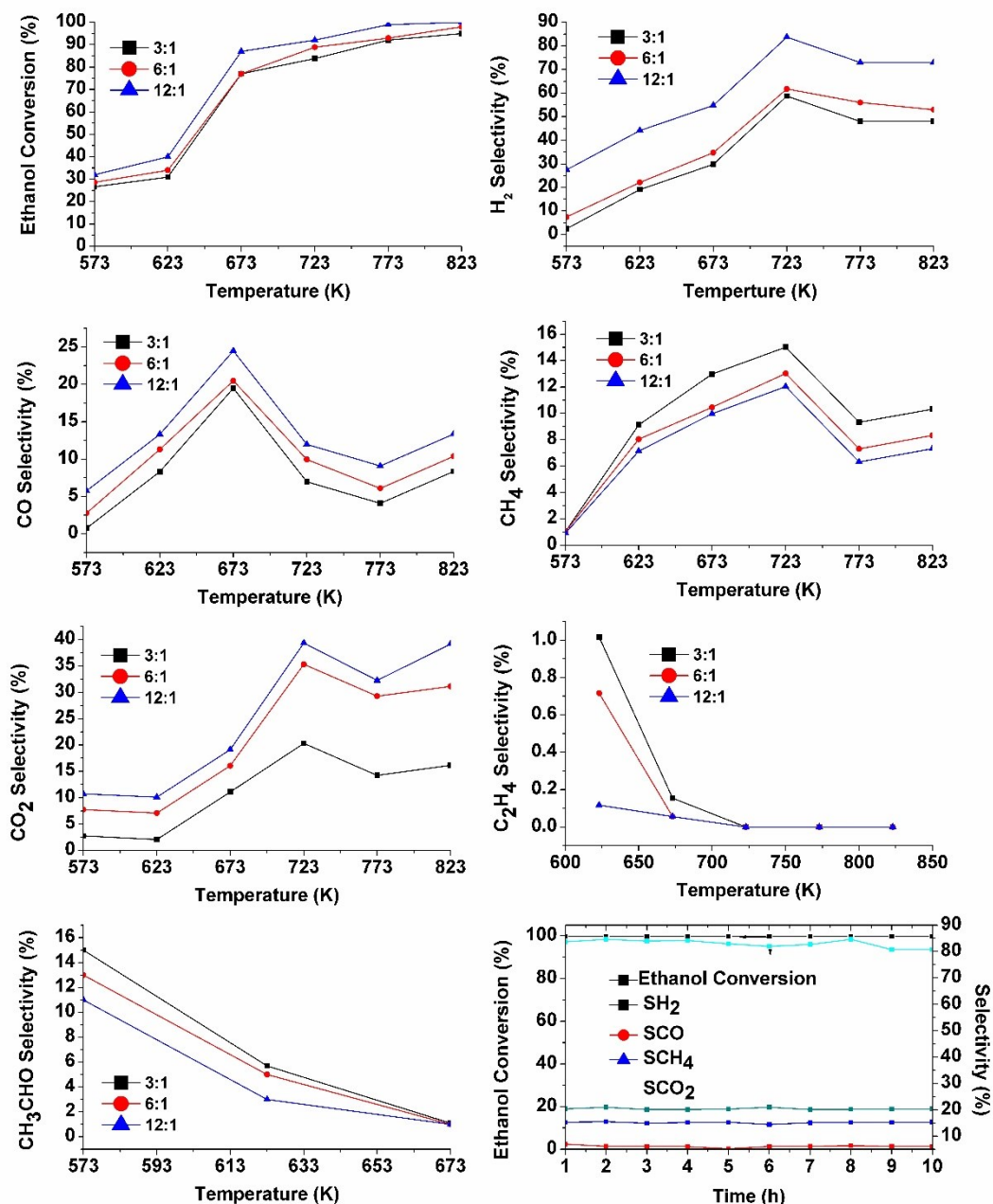


Figure 8.10 ESR performance and product selectivity with temperature.

The  $\text{CH}_3\text{CHO}$  formation was commonly observed for  $\text{CeO}_2$  based catalyst, but there is some contradiction regarding acetone or acetylene formation. Two different groups, Song et al. and Wang et al. [343, 360] reported the presence of acetone, whereas Machocki et al. and Loven et al. [67, 68] reported  $\text{C}_2\text{H}_4$  formation. Loven et al. have suggested the possibility of acid sites favoring the  $\text{C}_2\text{H}_4$  formation considering the work reported by Nishiguchi et al. [361]. The effect of particle size during ESR by Soyakal et al. [339] revealed that nano  $\text{CeO}_2$  facilitates the  $\text{C}_2\text{H}_4$  formation at each temperature. In present study as well as the work reported by Machocki et al. are based on nano  $\text{CeO}_2$  based support, the results are in agreement. Therefore, the acetone formation was completely absent in the liquid product for every catalyst. The product gas selectivity was almost similar to the bare Ni and Co catalysts as found in chapter 3. The notable point is in the presence of 20% active metals supported on  $\text{CeO}_2$ , the activity is equivalent to the bare active metals.

The optimization of water/ethanol ratio on 20Ni-Co/ $\text{CeO}_2$  catalyst for ESR was represented in Figure 8.11. From the figure it is clear that the ethanol conversion,  $\text{H}_2$  selectivity and  $\text{CO}_2$  selectivity get prominently increased with increase in the concentration of water in feed mixture. However, CO selectivity was also increasing but with less proportion. The selectivity of  $\text{CH}_4$  and  $\text{CH}_3\text{CHO}$  were significantly reduced by increasing the water content in feed mixture. It may be due to reformation of  $\text{CH}_4$  with water producing syn-gas and  $\text{CO}_2$  as described in chapter 1 by equations 1.22 and 1.23. The  $\text{C}_2\text{H}_4$  also reacts with  $\text{H}_2\text{O}$  forming CO and  $\text{CO}_2$  as described by eqs 1.18 and 1.19. Hence, the concentration of CO and  $\text{CO}_2$  both get increased by increasing the water concentration. The time on stream study suggested that the product gas distribution was stable up to 10 h duration.



**Figure 8.11** Selectivity of different product gases with variation in ethanol water molar ratio for 20Ni-Co/CeO<sub>2</sub> with temperature. Time on Stream study performed at 773K, Ethanol: water (12:1), WHSV= 35.4h<sup>-1</sup>.

#### 8.4 Conclusion

A substantial route of nano sized metal oxide is developed by using ethanol solvent and solvothermal treatment. This method was termed by us as a solvothermal precipitation and the catalyst prepared by this method was found highly active for ESR.